ANTITUMOUR ACTIVITY OF THE ERK DIMERIZATION INHIBITOR DEL-22379 IN LUNG ADENOCARCINOMA

MASTER IN MOLECULAR BIOLOGY AND BIOMEDICINE
UNIVERSITY OF CANTABRIA
2020/2021

ADRIÁN APARICIO REY

DIRECTOR: BERTA CASAR MARTÍNEZ
CODIRECTOR: PIERO CRESPO BARAJA

Transformation and Metastasis Department (IBBTEC)

ÍNDICE

1. ABSTRACT

Lung cancer is the leading cause of cancer-related mortality in both men and women worldwide. The most frequent type is lung adenocarcinoma, which accounts for 40% of all lung cancer cases. The RAS-RAF-MEK-ERK pathway (MAPK pathway) is known for being essential in cellular functions such as cell proliferation, differentiation, and apoptosis. Due to its important roles regulating cell functions, the MAPK pathway is commonly altered in many tumours, including lung adenocarcinomas. In the last years, numerous inhibitors of the cascade have been developed, and some of them have even progressed into the clinics. The most successful ones have been RAF and MEK inhibitors. However, patients treated with these drugs usually present relapses because of acquired resistance. For this reason, ERK has been recently considered as a potential target in cancer therapy, although *ERK* mutations rarely occur in tumours. In previous results from our laboratory, researchers have demonstrated that the prevention of ERK dimerization is a viable strategy to supress oncogenesis and tumour growth. Using a novel ERK dimerization screening method, Crespo et al. discovered a compound capable of effectively inhibiting ERK dimerization, which they called DEL-22379. This drug presented several antineoplastic properties in melanoma and colorectal cancer cells, such as generation of apoptotic response, a decrease of the tumour mass and lower metastatic spread. To further investigate the inhibitor's potential, the purpose of this study is to analyse the antitumour effects of DEL-22379 in lung adenocarcinoma, in both cell culture and chick embryo animal model.

2. BACKGROUND AND ACTUAL STATE OF THE TOPIC

2.1 Lung adenocarcinoma

Lung cancer is the most common cause of cancer-related deaths in men and women in the world (Barta et al., 2019). Its appearance has a strong association with cigarette smoking, but it is also linked to other risk factors, like ionizing radiation, environmental toxins, metals (arsenic chromium and nickel), history of pulmonary fibrosis, human immunodeficiency virus infection and alcohol consumption (Duma et al., 2019).

Most lung cancers are in an advanced stage when diagnosed, and consequently, the prognosis is very poor. More than 80% of patients with advanced lung cancer are dead by 5 years (Myers & Wallen, 2021), and the longevity of the patients has not increased over the past 3 decades. Therefore, screening and prevention are on the spotlight.

Symptoms and physical signs are dependent on the stage of lung cancer. The earliest stages are often asymptomatic, with nodules found incidentally on radiographic images testing for other disease processes. Later stage lung cancer usually exhibit symptoms such as a cough, hemoptysis, chest pain, dyspnea or unintentional weight loss (Duma et al., 2019).

Adenocarcinoma, a type of non-small cell lung cancer (NSCLC), accounts for approximately 40% of lung cancers (Barta et al., 2019), replacing the squamous cell lung cancer as the most prevalent non-small cell lung cancer in the last two decades. In patients, adenocarcinomas often stain positively with antibodies to markers of the alveolar type II cells, the surfactant-producing epithelial cells in the alveolar space, or the bronchiolar epithelial club (Clara) cells, the secretory cells lining the airways (Rowbotham & Kim, 2014). These cell types are thought to be responsible for tumour origin. Lung adenocarcinoma is classified into four subtypes: adenocarcinoma in situ, minimally invasive adenocarcinoma, invasive adenocarcinoma, and lepidic predominant adenocarcinoma (Lambe et al., 2020).

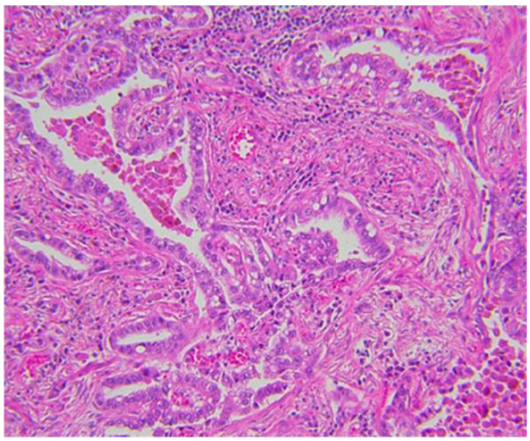

Figure 1. Minimally invasive adenocarcinoma histopathology. **(**H&E, 20×). *(Lambe et al., 2020).*

Over the last 40 years, there has been a marked increase in lung adenocarcinoma in women, and this has been linked to smoking. An immense majority of patients will have a smoking history and may have other associated factors such as chronic obstructive pulmonary disease or a family history of lung cancer (Myers & Wallen, 2021).

Local metastasis may involve spread directly to the pleura, diaphragm, pericardium, or bronchi with advanced disease spreading to the mediastinum, great vessels, trachea, esophagus, vertebral column, or adjacent lobe. Distant metastasis includes extension to a contralateral lobe, pleural nodules, malignant pleural or pericardial effusion, or any distant site such as the brain, bones, or liver (Myers & Wallen, 2021).

2.2The ERK1/2 signalling pathway

The ERK1/2 pathway (sometimes referred as the MAPK pathway) is one of most studied MAPK (mitogen-activated protein kinases) cascades (Degirmenci et al., 2020; Guo et al., 2020; Kidger et al., 2018; Liu et al., 2018; McCubrey et al., 2007). This pathway is well defined due to its relevance in essential cellular functions, such as cell proliferation, growth, differentiation, cell cycle regulation and apoptosis.

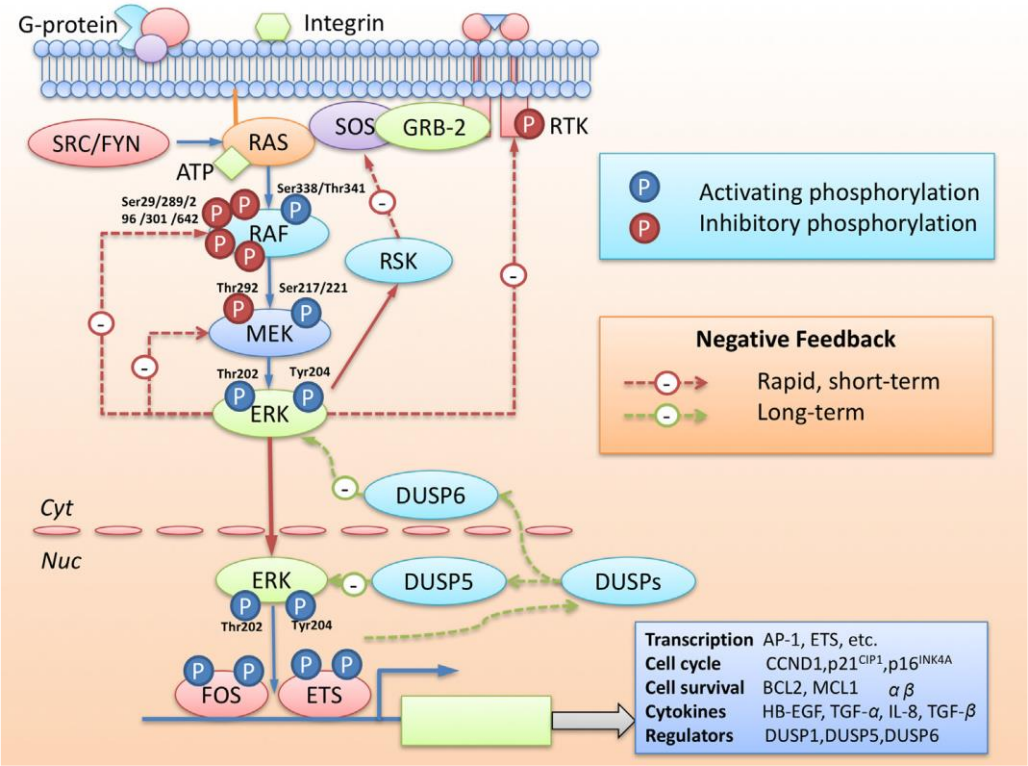

Figure 2. Structure of the MAPK pathway, representing the main components of the cascade and their interactions. *(Liu et al., 2018).*

The RAS-RAF-MEK1/2-ERK1/2 signalling pathway is activated by a large variety of extracellular molecules, like growth factors, cytokines, hormones, and neuropeptides. This molecules function as stimuli when they bind to their receptor in the cell extracellular membrane, mainly tyrosine kinase receptors (RTKs), initiating the cascade. After the receptors are activated, they dimerize and autophosphorilate themselves. This allows the activation of the growth factor receptor-bound protein 2 (Grb2), which forms a complex with son of sevenless 1 (SOS1), a

guanine nucleotide exchange factor. SOS interchange GDP for GTP in the RAS molecule, making it active and recruiting it into the plasma membrane, functioning as a binary on-off switch of the pathway.

RAS is a GTPase involved in numerous signalling routes, such as the ERK1/2 pathway. RAS superfamily includes over 150 small G-proteins, including K-RAS, H-RAS, N-RAS and others. When RAS is bound to GTP, it goes through a conformational change and is able to activate its downstream effector of the ERK1/2 pathway: RAF.

RAF is a protein with serine/threonine protein kinase activity when it is bound to RAS in the inner layer of the plasma membrane, where they can change their phosphorylation state, dimerize, and interact with scaffold proteins. In mammals, RAF kinase comprises three isoforms with different tissue distribution and level of kinase activity: A-RAF, B-RAF and C-RAF (or RAF-1). When RAF is activated, it can phosphorylate the next kinase of the route, MEK.

There are two MEK subtypes, MEK1 and MEK2. MEK is a dual specificity kinase that activates ERK by phosphorylating both of its Tyrosine and Threonine regulatory sites. ERK needs to be phosphorylated by MEK in the activation loop, which contains a characteristic TxY (threonine-x-tyrosine) motif or TEY motif. ERK is the last kinase of the pathway and, as its upstream activator MEK, has two isoforms: ERK1 and ERK2. They are serine/threonine protein kinases, which can activate a wide range of cytoplasmatic and nuclear substrates, like transcription factors, phosphatases, and cytoskeletal proteins. The signal also promotes ERK dimerization, which is necessary for the activation of certain cytoplasmatic substrates. These substrates participate in the control cellular metabolism, mitochondrial fission, and cell survival. On the other hand, ERK function in the nucleus is mostly performed as a monomer. In the nucleus, ERK can activate transcription factors such as CREB, c-Myc and NF-kB.

Although the RAS-ERK pathway is frequently described as linear and unidirectional, there are several interactions within the pathway and between other signalling networks that do not correspond with this description. One of the most relevant is the homeostatic control of the cascade by ERK using feedback loops. This regulation has rapid short-term effects, like ERK promoting the inhibition of upstream kinases like MEK, RAF and RTKs by phosphorylating certain residues. It can also produce a long-term feedback effect by stimulating the de novo expression of proteins like DUSPs, a dual-specificity phosphatase that inhibits the pathway by dephosphorylating ERK.

In addition, the pathway is modulated by multiple regulatory proteins. Scaffold proteins are the most abundant of this group. They are characterized for been capable of binding at least two members of the cascade, forming a functionally stable complex. Beside their assembly capabilities, scaffold proteins can act as allosteric stimulators to optimize signal flux. Therefore,

these proteins can regulate the duration, amplitude, and intensity of the signal, as well as the spatial specificity (Casar & Crespo, 2016).

To add more complexity to this pathway, RAS kinase can activate both MAPK and PI3K/AKT/mTOR pathway. Moreover, the dynamic interaction between RAS/ERK and RAS/PI3K cascades, by both positive and negative feedback loops, ensures the bidirectional communication with other pathways (Braicu et al., 2019).

2.3 The RAS-ERK pathway in cancer

The RAS-ERK signalling pathway is not only involved in physiological cellular processes, but the association of point mutations across the members within the cascade with tumour formation and poor prognosis has been described in numerous studies (**Table 1**).

Table 1. Frequency of mutations in the main components of the MAPK pathway across different tumours*. Adapted from Guo et al., 2020.*

Tumour type	*K-RAS*	*N-RAS*	*H-RAS*	*B-RAF*	*MEK*	*ERK*
Melanoma	15-29%	20%	-	90%	3-8%	67-90%
NSCLC	35%	-	-	4%	-	-
Colorectal	40%	-	-	5-20%	3%	-
High-grade serous ovarian cancer	0-12%	-	-	-	-	-
Low-grade serous ovarian cancer	27-36%	-	-	33-50%	-	-
Thyroid carcinoma	9-27%	9-27%	9-27%	10-70%	-	-
Papillary thyroid cancer	20%	-	-	-	-	-
Anaplastic/follicular thyroid cancer	-	15%	-	-	-	-
Hairy cell	-	-	-	79-100%	-	-
Pancreatic ductal adenocarcinoma	70%	-	-	-	-	-
Acute myleoid leukaemia	10%	-	-	-	-	-
Bladder urotherial carcinoma	-	-	20%	-	-	-
Renal cell carcnoma	-	-	2%	-	-	-
Breast cancer	5%	-	-	1%	7-9%	-

RAS is mutated in approximately one-third of all cancers, with high prevalence in pancreas (90%), colon (50%), thyroid (50%), lung (30%) cancers and melanoma (25%) (Fernández-Medarde & Santos, 2011). *RAS* mutations mostly occur in *K-RAS* (85%), followed by *N-RAS* (12%) and *H-RAS* (3%). Generally, mutated RAS proteins are constitutively bound to GTP. This leads to the continuous activation and phosphorylation of downstream effectors, with high levels of p-MEK and p-ERK.

RAF was not considered a relevant cancer driver gene until the discovery of the *B-RAF(V600E)* mutation in 2002. This mutation represents more than the 90% of all *RAF* mutation events in cancer cells genomes, *C-RAF* and *A-RAF* mutations are much less common (Degirmenci et al.,

2020). The mutations can cause different effects, like simulating phosphorylated state, disrupting the auto-inhibitory conformation, or activating the wild-type RAF counterparts.

In contrast to RAS and RAF mutations, MEK mutations are considerably less frequent in cancer cells, but can act as cancer drivers. The mutations can interrupt the auto-inhibitory state or enhance MEK homodimerization (Degirmenci et al., 2020).

Finally, ERK mutations rarely occur in cancers. $ERK2^{E322k}$ mutation has been detected in significant cases of cervical, head and neck squamous cell carcinomas. The mutated protein exhibits higher levels of activity due to defects in DUSP binding site, remaining in a phosphorylated state (Kidger et al., 2018).

All these mutations ultimately lead to the persistent and increased activation of the RAS-ERK pathway, which is closely related to the occurrence and development of tumours. This activation can promote cellular functions typical of cancer cells. For example, it can stimulate proliferation and inhibit apoptosis by influencing the activity of cell cycle regulatory proteins and apoptosis-related proteins in cancer cells (Maemura et al., 2009). RAS-ERK signalling pathway activation can also lead to increased tumour invasion and metastasis capabilities by favouring the degradation of the extracellular matrix, cell migration and angiogenesis (Guo et al., 2020). Due to the importance of the pathway in tumours, the efforts made to understand the working mechanisms of the cascade and to target its components in cancer cells have grown in the last years.

2.4 RAS-ERK pathway alterations in lung adenocarcinoma

About 20-30% of lung adenocarcinomas present a mutation in the *RAS* gene. In fact, adenocarcinomas cases are the NSCLCs with higher frequency of *K-RAS* mutations than other subtypes (Boch et al., 2013). These mutations have been correlated with clinical and pathological characteristics of the patient, being more common in females and smokers. Furthermore, there are numerous evidences supporting that oncogenic K-RAS signalling, through the RAS-ERK pathway, can drive histological progression of adenomas to malignant carcinomas. (Cicchini et al., 2017). Other less prevalent *RAS* mutations, like in *N-RAS*, can be useful to foresee clinical and therapeutic features of the tumours.

Mutations of the *B-RAF* proto-oncogene are common in melanomas but can also occur less frequently in other cancer types, like lung adenocarcinoma. *B-RAF* is mutated in approximately 4% of all NSCLCs (Guo et al., 2020).

The epithelial growth factor receptor (EGFR) is a glycoprotein present in plasma membrane that can be stimulated by ligand such as EGF, TFGα or neuregilins to activate the MAPK pathway

and stimulate cellular proliferation (Bethune et al., 2010). When the ligand binds to EGFR, it dimerizes and phosphorylates itself, initiating the signalling cascade. Deregulation of EGFR has been observed in 40-89% of NSCLCs. Interestingly, it has been reported that the mutations that cause gain of function of both proto-oncogenes *K-RAS* and *EGFR* are mutually exclusive in lung adenocarcinomas, a phenomenon that can be explained by synthetic toxicity, which induces cell death (Unni et al., 2018).

2.5 Current status of MAPK pathway inhibitors in cancer therapy

Since the RAS-ERK pathway presents a wide variety of alterations in cancer genomes, it has attracted the interest of cancer researchers. Every protein of the cascade represents a potential druggable target to inhibit to stop signal propagation. In the last years, an enormous effort has been made by biomedical scientist to discover new compounds able of inhibiting the components of the MAPK pathway, in order to prevent tumour growth and propagation.

The development RAS inhibitors has supposed a significant challenge, mostly due to the high GTP affinity of the mutants, which prevents GTP hydrolysis, and the lack of a binding pocket for small molecule inhibitor binding (Cox et al., 2014). For these reasons, and for a long period of time, RAS protein was believed to be undruggable. Nonetheless, recent novel approaches have been developed to overcome these problems. For example, one of the strategies consist in targeting proteins that regulate RAS-GTP interaction, like SOS, which is a regulator of GDP/GTP exchange of RAS. Another promising alternative seems to be the inhibition of the functionally relevant post-translational modifications, like prenylation. In the case of lung adenocarcinomas, it has been reported that small molecule compounds (SML-8-73-1 and SML-10-70-1) can inhibit K-RAS G12C mutant (Lim et al., 2014). This mutation is present in almost half of RAS-driven lung adenocarcinomas. Despite the efforts made, the aforementioned approaches are limited to laboratory models, and the development of effective molecules showing clinical effectiveness is still far from the present.

RAF, as the first kinase of the cascade, has been considered a valuable target against cancer. One of the first discovered molecules capable to inhibit RAF was Sorafenib, an orally available compound. It was originally described as a C-RAF isoform inhibitor, and later identified as a multikinase inhibitor. Sorafenib can inhibit angiogenesis and tumour growth, and has preclinical and clinical activity against certain types of cancers (for example, ovarian, breast and pancreatic cancer) (Fucile et al., 2015). Other first-generation RAF inhibitors include Vemurafenib, Dabrafenib and Encorafenib. NSCLC patients harbouring the *B-RAF V600E* mutation have shown a good response to dabrafenib (Anguera & Majem, 2018). More recently, it has been observed that genetic ablation of *C-RAF* in *K-RAS* driven tumours induced significant rates of tumour regression in lung adenocarcinoma, suggesting that the inhibition of the activity or

expression of C-RAF might be a suitable therapeutic option (Drosten & Barbacid, 2020). Despite of the initial achievements of these drugs, tumours quickly develop resistance, leading to tumour progression and relapses (Degirmenci et al., 2020). Cancer cells can acquire resistance through two different mechanisms. First, they can increase the expression of the RAS protein, which leads to what is known as "paradoxical activation" of the RAS-ERK pathway. Secondly, the generation of a splicing variant of B-RAF(V600E) can enhance its dimerization and activity. Curiously, resistant cancer cells become drug-dependent, and dray withdrawal inhibits their growth and proliferation. To overcome the appearance of resistant tumours, a second generation of RAF inhibitors was developed.

Because of their low mutation frequency in human cancers, MEK1/2 kinases were not considered acceptable targets against tumours. However, the emergence of resistance to RAF inhibitors, the interest in this kinase has grown among researchers. The first reported MEK1/2 inhibitor was PD098059, which can inhibit the dephosphorylated state of MEK1. U0126 and its high inhibition specificity towards MEK were discovered some years later, but its poor pharmacological properties relegated this drug as a research tool (Frémin & Meloche, 2010). PD0325901, an allosteric inhibitor that stabilizes the inactive conformation of MEK1/2, was one of the first inhibitors to reach clinical trials (Kohler et al., 2018). The use of MEK inhibitors in combination with RAF inhibitors was found to be quite effective, especially in metastatic melanoma. Moreover, a significant number of studies have reported preclinical evidence of the effectiveness of MEK targeting therapies in NSCLC using inhibitors like Selumetinib and Trametinib (Abdel-Rahman, 2016). However, like their RAF counterparts, MEK inhibitors rapidly generate drug resistance in treated cancer cells, both for monotherapy and combination therapy (Liu et al., 2018). There are several mechanisms that allow cancer cells to respond against MEK targeted therapy, like the overactivation of upstream intermediaries of the pathway, *MEK* mutations, activation of parallel signalling pathways, transcription factors regulation, etc. In addition, due to their high ligand affinity, many MEK inhibitors also affect and non-cancerous cells in a considerable proportion, resulting in high toxicity and clinical limitations.

EGFR inhibitors have also been used in cancer therapy. These molecules bind to EGFR, blocking the binding of alternative ligands, preventing the initiation of the signalling pathway (Pradhan et al., 2019). Approval of tyrosine kinase inhibitors such as Erlotinib, Gefitinib, and Lapatinib for the treatment of non-small cell lung cancer led to tremendous development of novel EGFR inhibitors in the last decade. In fact, there are numerous preclinical studies showing the synergistic effects of EGFRi and MEKi combination therapy against NSCLC (Abdel-Rahman, 2016), significantly reducing the generation of MEKi or EGFRi resistant tumours. However, almost all lung cancer cases experience disease recurrence after one to two years, mostly due to EGFR mutations that generate acquired resistance (Nagano et al., 2018).

Despite the initial successes of these kinase inhibitors, the apparently unavoidable drug resistance has emerged as the main problem when targeting the MAPK pathway in cancer. This resistance usually appears as a consequence of the activation of upstream elements of the cascade through various mechanisms. Hence, targeting the most downstream kinase of the pathway was considered as viable alternative. Although *ERK* gene is rarely mutated in cancer cells, therapeutical inhibition of this kinase has several advantages.

First, every alteration of the RAS-ERK pathway in cancer cells ultimately leads to the overactivation of ERK, which then is able to stimulate a wide variety of substrates. ERK1/2 receives the information from MEK, which previously acquired it from RAF, and the passes it on to multiple targets. Thus, ERK1/2 can be seen as the bottleneck of the pathway. Therefore, when we consider the structure of the cascade, the inhibition of the last effector of the cascade seems the most optimal approach.

Secondly, ERK inhibition can overcome the drug resistance originated by upstream kinases inhibitors. As it has been explained before, the acquired resistance to EGFR, RAF and MEK inhibitors implies the reactivation of the MAPK pathway by a series of mechanisms previously mentioned. It has been reported that selective ERK inhibitors can reverse this resistance (Liu et al., 2018). Moreover, it is believed that these inhibitors are less prone to generate drug resistance.

As described before, the MAPK pathway presents negative ERK-dependent feedback loops that regulate the pathway. This results in the inhibition of RAF, MEK and RTK activity. However, when cells are treated with inhibitors that target these upstream kinases, they lose the regulation caused by the feedback loops, which leads to their subsequent activation and the reinstallation of the signal (Kidger et al., 2018). This rebound is considerably stronger in cells carrying *RAS* mutations. If ERK is inhibited, the ERK-dependent feedback loops are also supressed.

For all these advantages, a significant amount of small molecule inhibitors of ERK1/2 have been discovered and studied recently. Some have even progressed into clinical trials. There are many different types of ERK inhibitors.

Reversible ATP-competitive ERK1/2 inhibitors attach to the active or inactive conformation of the ATP-binding pocket. Many of these drugs, including BVD-523 (Chin et al., 2020), also known as Ulixertinib, GDC-0994 and SCH772984 (Kidger et al., 2018), are now in clinical trials. Both are ATP-competitive inhibitors that suppress cell proliferation in cell lines with B-RAF or K-RAS mutations. SCH772984 has been demonstrated to efficiently suppress both ERK1/2 catalytic activity and its phosphorylation by MEK1/2. The effectiveness of BVD-523 was also assessed in Vemurafenib-resistant patient-derived xenografts. It is also in phase I/II clinical studies for solid tumours and melanoma that resist RAF and MEK inhibitors.

Another type of inhibitors is the covalent ERK1/2 inhibitors. They bind to their target protein forming a covalent interaction that can be reversible or irreversible (Kidger et al., 2018). Because the covalent interaction results in either a very slow off-rate for the inhibitor or a permanently inhibited target protein, de novo synthesis of the target is required to re-establish activity, this method of inhibition is proposed to facilitate prolonged inhibition of the target protein and with high potency. Examples of these drugs include Afatinib, Neratinib, Ibrutinib and Osimertinib. Nonetheless, because of their intrinsic reactivity, covalent inhibitors may have off-target effects by interacting with cysteines and other reactive residues across the proteome. This makes it difficult for them to achieve success in clinical trials.

A newer approach consists in the development of allosteric ERK1/2 inhibitors, which attach at locations other than the catalytic cleft and prevent ERK1/2 from interacting with its binding partners (Yap et al., 2011). The first small molecule allosteric ERKi was discovered in more than 15 years ago, using computational design (Hancock et al., 2005). This type of inhibition allows the molecules to supress ERK phosphorylation, prevent dimerization, or selectively block the attachment to its substrates.

In clinical studies, selective ERK inhibitors have been used to treat a great range of malignancies, the most prevalent of which are advanced solid tumours with MAPK pathway abnormalities. Melanoma, pancreatic adenocarcinoma, and non-small cell lung cancer were the most prevalent solid tumour malignancies treated in these clinical trials (Chin et al., 2020). There are several studies that support the therapeutic potential of ERK inhibitors in lung cancer. ERK inhibitors were used in Gefitinib (an EGFR inhibitor used to treat NSCLC patients) resistant cancer cell, successfully reverting this resistance (Qi et al., 2018). This was also verified for another EGFRi, Osimertinib (Li et al., 2020). A different ERKi, LY3214996, has shown promising results in experiments using patient-derived xenograft models of RAS-mutant lung cancer (Köhler et al., 2021).

Unfortunately, as observed with other MAPK pathway inhibitors, treatment with ERK inhibitors can also cause resistance in the clinic. Mutations in ERK1/2, ERK2 amplification and overexpression, and EGFR increased expression levels have all been identified as mechanisms of acquired resistance in resistant cell lines (Jaiswal et al., 2018). Moreover, ERK inhibitor resistant lung cancer cell lines have been generated in the laboratory. For example, Iezzi et al. created a SCH772984 resistant NSCLC cell line (Iezzi et al., 2018).

To avoid resistance, combining ERK1/2 inhibitors with other kinase inhibitors seems a promising therapeutical approach, as in the case of RAFi. In B-RAF (V600E) melanoma, B-RAFi and ERKi combination is likely to be more effective and well tolerated than B-RAFi alone, as is the case with B-RAFi and MEKi combination (Kidger et al., 2018). In fact, the combination of MEK and

ERK inhibitors has been tested in lung adenocarcinoma A549 cells, where the mixed treatment of Cobimetinib (MEKi) and GDC-0994 (ERKi) significantly diminished tumoral activity *in vivo*, reducing the tumour growth in a synergic way (Merchant et al., 2017). Although in this particular experiment the doses where well tolerated by the animals used, for most of the cases the difficulty resides in balancing inhibitor synergy in the tumour cell with the increased toxicity caused by action in non-tumour tissue.

2.6 Progress in Piero's laboratory

In previous studies in Piero's laboratory, they discovered that ERK1/2 dimers and scaffolds are essential for optimum activation of cytoplasmic substrates. In fact, inhibiting ERK1/2 dimerization can stop tumour cell proliferation *in vitro*, and oncogenesis and tumour development *in vivo* (Casar et al., 2008). This research established ERK1/2 dimerization as a possible target in tumours and opened new pathways for developing new ERK inhibitors.

As a result, Herrero and colleagues devised a native gel electrophoresis method for screening of ERK1/2 dimerization inhibitors (Herrero et al., 2015). DEL-22379 (**Figure 3**), a 3-arylidene-2-oxindole derivative, was identified as a small molecule capable of inhibiting ERK1/2 dimerization while having no effect on ERK1/2 phosphorylation or catalytic activity in the tested cell lines. The DEL-22379 binding site on ERK2 is located in a cleft near the dimerization interface, adjacent to important dimerization residues such as His 176. This prevents the interaction between two ERK molecules.

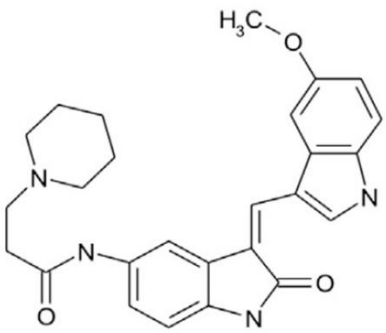

Figure 3. Structure of DEL-22379. *(Herrero et al., 2015)*

In this same study, it was demonstrated that DEL-22379 inhibited the phosphorylation of ERK1/2 cytoplasmic substrates as well as the proliferation of RAS-ERK pathway oncogene-expressing tumour cell lines and xenografts. In xenografts from melanoma and colorectal cancer cell lines containing mutant B-RAF and RAS, DEL-22379 causes a significant apoptotic response, as well as a reduction in primary tumour mass and metastatic spread.

Moreover, the inhibition of tumour growth by DEL-22379 was not affected by classical RAS-ERK pathway inhibitor resistance mechanisms. DEL-22379 had the same antiproliferative effect in A375 melanoma cells which overexpressed a mutated N-RAS, as opposed to the failure of B-RAF inhibitor PLX-4032. Similar results were found in another experiment with HT29 colorectal cancer cells overexpressing B-RAF (V600E), where MEK inhibitor PD-0325901 treatment was unsuccessful and cells remained sensitive to DEL-22379.

3. OBJECTIVES

To further investigate DEL-22379 capabilities of inhibiting ERK dimerization, we inspected the effects of this drug in lung adenocarcinoma cells, both *in vitro* and *in vivo* conditions*.

To achieve this goal, A549 human lung adenocarcinoma cells were used, which are known to have a *K-RAS* mutation, while the *EGFR* is wild type. These cells have been used by other researchers as a model to study *K-RAS* driven lung tumours.

Our initial hypothesis was that DEL-22379 can inhibit ERK dimerization in A549 cells. If this premise turned out to be true, similar effects in the molecular dynamics of the pathway and in the neoplastic capabilities, previously observed in experiments carried by Herrero et al., were expected to appear in A549 cells. This could define DEL-22379 as a potential therapeutic agent in lung adenocarcinoma. Thus, the next objectives arose to give a response to these questions:

- Characterize the biochemical effects of DEL-22379 in A549 cells. ERK dimerization was examined, as well as the phosphorylation state of ERK. The activation or inactivation of different ERK substrates and other components of the pathway was also investigated.
- Compare the survival, migratory and invasive capabilities of DEL-22379-treated and non-treated A549 cells *in vitro*.
- Analyse the consequences of DEL-22349 treatment in A549 tumours *in vivo*, using the chick embryo animal model.

To determine the efficacy of DEL-22379 as an inhibitor in these cancer cells, two other inhibitors (U0126 and PD-0325901) were used to compare their activity and efficacy with those presented by DEL-22379.

*Because cells react to drugs differently in cell culture and in animal models, a distinction is made along this work. Experiments performed in cell cultures are considered *in vitro* conditions, while experiments using the chick embryo model are described as *in vivo*.

4. MATERIALS AND METHODS

4.1 Cell culture

A549 cells were cultured in Dulbecco's Modified Eagle's Medium (DMEM) supplemented with 10% fetal bovine serum (FBS) and 1% penicillin/streptomycin on a regular basis. When plates were confluent, they were washed with phosphate buffered saline (PBS) and detached using the appropriated volume of Trypsin/EDTA. Cells were kept in an incubator at 37 ° C, with 5% CO_2 and 98%relative humidity.

4.2 Treatment with inhibitors

To analyse the effects of each drug in lung cancer cells, A549 cells were previously starved for 24 hours using serum-free DMEM. Then, they were incubated with the drug, which were dissolved in dimethyl sulfoxide (DMSO), for one hour. EGF (Epidermal Growth Factor, SIGMA) has been used to stimulate cells at 50 ng/mL final concentration for 5 minutes.

4.3 Protein isolation

To get a total protein extract from cell cultures, the plates were placed on ice and washed with PBS 1X to remove any residues. Then, 200-250µL of lysis buffer was added to each culture plate. The buffer contained 20mM HEPES pH 7.5, 10mM EGTA, 40mM β-glycerolphosphate, 1% of not ionic detergent NP40, 2.5mM MgCl2, 2mM orthovanadate, 1mM DTT (dithiothreitol) and proteases inhibitor (10µg/mL aprotinin and 10µg/mL leupeptin). Lysates were collected and centrifugated at 13000 rpm during 10 minutes at 4ºC. Supernatants containing proteins were separated from the pellet after centrifugation.

4.4 Protein concentration measurement

The colorimetric technique of Bradford with the DCTM (Detergent Compatible) Protein Assay kit from Bio-Rad was used to measure and determine protein concentration. Subsequently, to 5µL of total protein extract, 25µL of a 50:1 mixture of Protein Assay Reagent A and Protein Assay Reagent S were added. Then, 200L of Protein Assay Reagent B were combined with the mixture. After that, the solution was incubated for 10 minutes at 37°C.

4.5 Immunoblotting

Samples were mix with 4X Laemmli buffer (100mM Tris pH 6.8, 4% SDS, 20% glycerol, 20mM DTT and 0.005% bromophenol blue) in a 1:4 ratio (Laemmli:sample). Then, they were heated at during 95ºC 5 minutes. The mix was placed in the well of a polyacrylamide gel, which was

composed of a stacking part (composed of 4% acrylamide, 125 mM Tris-HCl pH 6.8, 0.4% sodium dodecyl sulfate (SDS), 0.1% Ammonium Persulfate (APS) and 0.1% Tetramethyl ethylenediamine (TEMED) in H_2O) and a resolving part (the acrylamide percentage range was from 8% to 12% depending on the molecular weight of the protein, 375 mM Tris-HCl pH 8.8, 0.4% SDS, 0.1% APS and 0.1% TEMED in H_2O). Proteins were separated by size by SDS polyacrylamide gel electrophoresis (SDS-PAGE). The vertical electrophoresis separation took around one hour at 120V in a Mini-protean Bio-Rad equipment with running buffer (25 mM Trizma base, 192 mM Glycine, 0,1% SDS). The proteins were then transferred to nitrocellulose membranes in transfer solution (25 mM Trizma base and 192 mM Glycine) at 400 mA constant amperage under refrigerating conditions. The membranes were incubated with blocking solution (4% bovine serum albumin or BSA). Then, two ten minutes washes were performed in TBS-T at room temperature and shaking. After blocking, the membranes were incubated with the primary antibody (diluted in TBS-T 4%BSA) for 1-2 hours or overnight. Another two washes were performed before secondary antibody incubation (TBS-T 4% milk). The secondary antibodies used were conjugated with peroxidase enzyme for enhanced chemiluminescence detection (ECL). For this the membrane was previously washed and treated with solution 1 (1 M Tris HCl pH 8.5, 90 mM Coumaric Acid, 250 mM Luminol) and solution 2 (1 M Tris HCl pH 8.5, 30% Hydrogen Peroxide).

Table 2. Primary antibodies used in this work.

Antibody	*Specificity*	*Dilution*	*Reference*
Anti-ERK2	Mouse monoclonal	1:1000	sc-1647
Anti-p-ERK	Mouse monoclonal	1:4000	sc-7383
Anti-ERK1/2	Mouse monoclonal	1:1000	sc-514302
Anti-p-RSK1	Rabbit monoclonal	1:1000	Millipore: 04-419
Anti-RSK1	Rabbit monoclonal	1:1000	sc-231
Anti-p-ELK1	Rabbit monoclonal	1:1000	Cell signalling: 9181
Anti-ELK1	Rabbit monoclonal	1:1000	Cell signalling: 9182
Anti-p-MEK	Rabbit monoclonal	1:1000	Millipore: 07-852
Anti-MEK	Rabbit monoclonal	1:1000	Cell signalling: 8727S
Anti-p-RAF	Rabbit monoclonal	1:1000	sc-7267
Anti-alpha tubulin	Mouse monoclonal	1:1000	ABT171

4.6 ERK1/2 dimers detection

To detect dimerization of ERK, electrophoresis of the total cell lysate under native conditions was carried. This was achieved mixing the lysate with a specific loading buffer (0.126 M Tris HCl pH

6.8, 20% Glycerol, 0.1% Bromophenol blue). Employing SDS-free running buffer, samples were run in an 8% acrylamide gel without SDS at 80 V continuous voltage for one hour and a half. Membrane transfer was performed at 400mA for 80 minutes. The stages that follow are the same as those outlined in the Immunoblotting methodology.

4.7 Measurement of proliferation and survival rates

A549 cells were plated at 30,000 cells/well density in 24-well plates, washing and adding new drug every 24 hours. In order to quantify cell number, cells were washed with PBS and detached from the plates with Trypsin/EDTA. Cells were counted in a Neubauer Chamber at different times (24, 48, 72 and 96 hours). For these cells were mixed with Tripan Blue at a 1:1 ratio to differentiate dead cells from the others. The data was imported into GraphPad Prism, where it was normalized to a percentage of the control. All samples were triplicated.

4.8 IC_{50} calculation

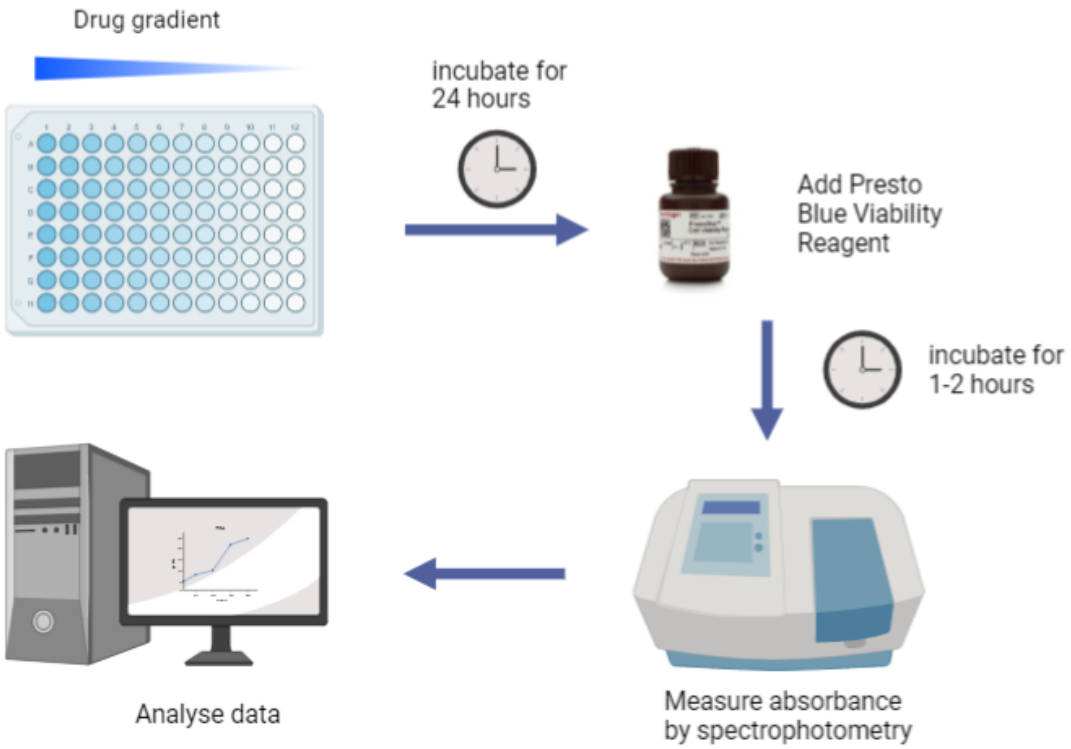

Figure 4. Scheme of the general steps followed for the determination of IC_{50} using a viability assay in A549 cells.

A549 cells were plated at 3,000 cell/well density in 96-well plate. Cells were treated with a gradient of drug concentration, except the control wells. All samples were triplicated. After 24 hours, 10µL of Presto Blue Viability Reagent (Invitrogen) was added to each well. Presto Blue Cell Viability Reagent is a prepared resazurin-based solution that acts as a cell health indicator

by quantifying viability using the reducing power of live cells. When resazurin enters live cells, it is converted to resorufin, a red molecule with a strong fluorescence. After1-2 hours of incubation at 37ºC, the absorbance was measured at 540nm and 620nm using a spectrophotometer. The 540nm/620nm index was calculated in Excel. The values were exported to GraphPad Prism and were normalized to a percentage of the control. The IC_{50} was calculated and the graphical representation of the experiment was performed using the same software

4.9 Preparation of cells for confocal fluorescence microscopy

For migration assays, cells were previously marked with Cell Tracker Green (Invitrogen), a fluorescent dye well suited for monitoring cell movement or location. Starved cells were incubated with 10 µL of a 10mM solution of the dye for one hour. Then cells were washed and 10% FBS DMEM was added for 30 minutes. After that, cells were trypsinized and counted. After the assay, fixed cells were treated with a solution of Hoechst 33258 (blue) to mark cell nucleus, and phalloidin (red) to mark cell cytoskeleton in a 1:100 PBS solution.

4.10 Cell migration analysis

The assay was performed using Transwells, which contained a polycarbonate membrane with an 8µm pore. The cells could migrate through the pore to the other side of the membrane. A549 cells were plated at 50,000 cells/well density and 150 µL of serum-free DMEM was added. 500 µL of DMEM containing 5% FBS was added to the down-compartment. After 24 hours, cells were washed in PBS, and then cells in the upper side of the transwell membrane where removed. The remaining cells were fixed using 4% paraformaldehyde (PFA). Another wash was performed before staining the cells with methyl violet. After ten minutes, the wells where washed several times in PBS. Lastly, the methyl violet was removed from the cells using an acetic acid solution, which was used for quantification. The absorbance of every condition was measured using a spectrophotometer (540nm). To evaluate the results and statistical significance of experimental groups, Graph Pad Prism software was used to normalize the results and to perform a Student T-test for each condition. The absorbance of each sample (two per condition) was measured twice.

4.11 Cell invasion analysis

Previously, the transwell membranes were covered with 50µL of matrigel resuspended on serum-free DMEM (1:20). A549 cells were plated at 50,000 cells/well density and 150 µL of serum-free DMEM was added. 500 µL of DMEM containing 5% FBS was added to the down-compartment. After 48 hours, cells were washed in PBS, and then cells in the upper side of the transwell membrane where removed. The rest of the steps were similar to the cell migration analysis protocol.

4.12 Preparing tumour cells for grafting

The cells were removed from their culture dishes using trypsin/EDTA after being washed twice in PBS 1X to eliminate any remaining medium. Neubauer Chamber was used to count the cells, which were then resuspended at 40 million cells/ml (10^6 cells/0,025L) in serum-free DMEM.

4.13 Chicken embryo xenografting

Freshly fertilized chicken eggs (Gibert Farm Tarragona, Spain) were incubated for 10 days at 37 degrees Celsius and 60% humidity, rotating every 30 minutes. The eggs were put horizontally on an eggcup on day 10. The top of the egg was disinfected using povidone-iodine. Then, the egg was pierced at the air sack side using a 30-gauge syringe needle After that, a little perforation of the eggshell was made using Dremel rotary tool kit. It was important that this hole penetrated the eggshell but not the CAM. Afterwards, a third extremely small hole in the eggshell membrane was made with a 20-gauge syringe needle with a little hook on the end. To lower the CAM and separate it from the top, liquid was vacuumed at the air sack hole using an automatic pipette aid fitted with a piece of Tygon tubing. Then, eggshell fragments were removed to make a small window at the top to expose the underlying CAM. A micropipette was used to place 25 µL of cell suspension over the exposed CAM. To allow the cells to settle, the window in the egg was securely covered with laboratory tape and the eggs were left with the embryos standing upwards for a few minutes. The eggs were then placed on an egg rack in a stationary incubator at 37 degrees Celsius and 60% relative humidity. For a macroscopic tumour to appear, cells were allowed to develop for 2 days. When the tumour was visible, they were treated with 25 µL of a 1:100 drug or vehicle dilution in PBS1X. The embryos were treated again after 24 hours.

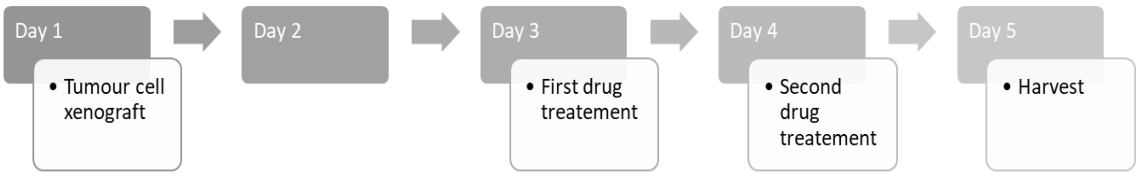

Figure 5. Experimental planning scheme of chick embryo xenografting*. At day 1 of the experiment, fecundated eggs had been incubated for10 days.*

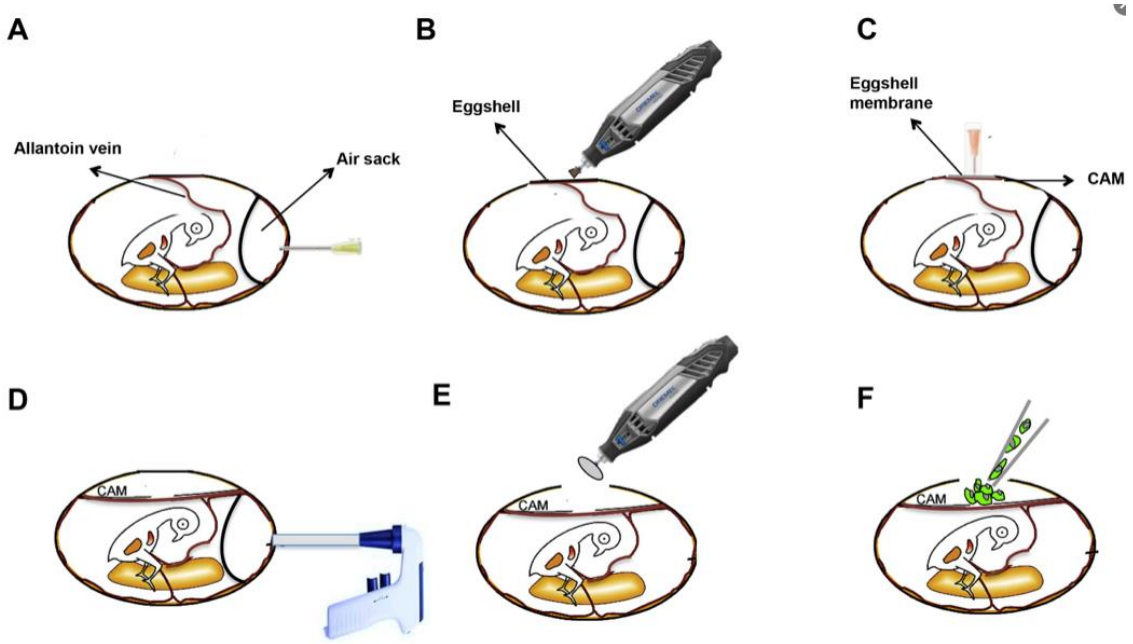

Figure 6. Overview of the main stages of the preparation of eggs for tumour cell xenografting. *(Crespo & Casar, 2016).*

4.13 Harvesting tumours and chick embryo tissues

At the fifth day, the primary tumour is detached from the CAM and weighed. They were maintained in 500 µL of 4% PFA at 4ºC. After one day, they were stored at -20ºC. The chick embryo was separated from the eggshell using a radial cut, and the embryo was deposited into a clean weight basket. The head was cut from the rest of the body through the neck. The embryo was dissected with sterile equipment. The CAM, the brain, the liver, and the lungs were collected in pieces and placed in microcentrifuge tubes. After extraction, organs were stored at -20ºC.

4.14 Genomic DNA isolation

Samples were added 600 µL of Cell Lysis Buffer (Qiagen) with 0.03% of proteinase K. For chicken embryo organs, samples were disaggregated using Polytron. The samples were then incubated overnight at 60ºC. The next day, 200 µL of protein precipitation solution was mixed with the samples. After a 5-minute centrifugation at 13000 rpm, supernatant was rescued, and isopropanol was added at 1:1 ratio. A few minutes after, another 5-minute centrifugation at 13000 rpm was performed. Supernatant was discarded and the genomic DNA pellet was washed three times using 70% ethanol. After the final centrifugation, the pellet was completely dried. Finally, it was resuspended in 200 µL of hydration solution. The genomic DNA was quantified using Nanodrop (Thermo Scientific). 1 µL of DNA was used for the quantification.

4.15 RT-qPCR analysis

The PCR was carried out in a total reaction volume of 20 µL, comprising 19 µL of SYBR Select Master Mix (Applied Biosystems) with ultrapure water (1:1), 20 ng of genomic DNA, and 0.05 µL of each ALU primer (sense: 5'-ACGCCTGTAATCCCAGGACTT-3'; antisense: 5'-TCGCCCAGGCTGGCTGGGTGCA-3'). A standard curve was created utilizing a dilution of human DNA from the A549 cells (10^2, 10^3, 10^4) as a positive control and water as a negative control. All samples had duplicates. The PCR was performed at 95°C for 2 minutes, followed by 40 cycles of 30 seconds at 95°C, 30 seconds at 63°C, and 30 seconds at 72°C. Ct values were extrapolated to the standard curve to determine the number of tumour cells present in brain, CAM, lung, and liver samples. A Student T-test was performed to examine the results and statistical significance of the control and experimental groups using Graph Pad Prism software.

5. RESULTS

5.1 DEL-22379 inhibits ERK dimerization without affecting its phosphorylation in A549 cells

First, to make sure DEL-23379 stock maintained its properties, a small experiment was performed using human embryonic kidney HEK 293T cells (**Figure 7**). To check it, native electrophoresis was performed using the total lysates of the cells, previously treated with DEL-22379 for one hour and stimulated with EGF for 5 minutes. The inhibitor could avoid the formation of dimers as observed in previous studies (Herrero et al., 2015). The next experiment (**Figure 8**) consisted in finding out if DEL-22379 could prevent ERK dimerization in lung adenocarcinoma human A549 cells. Cells were treated with different concentrations of the drug.

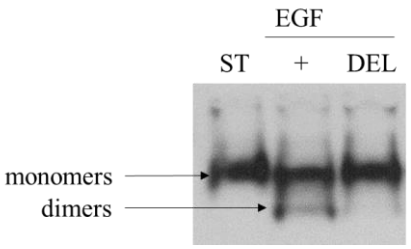

Figure 7. DEL-22379 prevents ERK dimerization in HEK 293T cells. *A cell plate was left with no EGF stimulation (ST). DEL-22379 (DEL) concentration used was 10 µM. Membrane was incubated with anti-ERK2 primary antibody.*

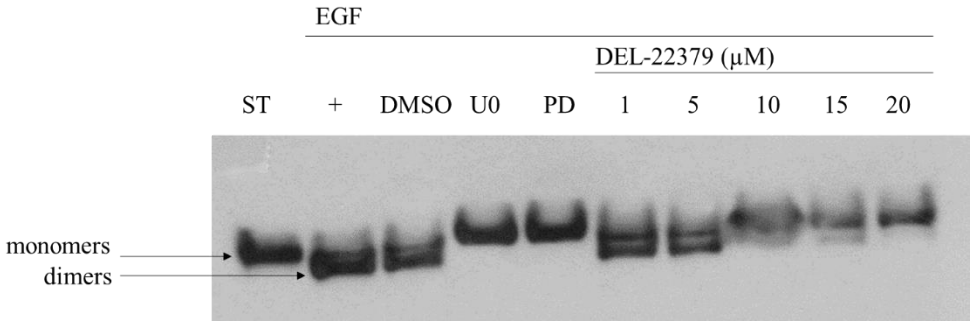

Figure 8. ERK dimerization analysis in A549 cells using native gel electrophoresis*. The dimer runs faster in the gel because it has a greater negative charge and dipole moment, due to the embedding of charged residues during dimerization. DMSO was used as a vehicle for the drugs. U0 (U0126) and PD (PD-0325901) were used at a final concentration of 10 µM. DEL-22379 was used at the indicated µM final concentrations. Membrane was incubated with anti-ERK2 primary antibody.*

EGF treatment of A549 cells stimulated the propagation of the signal and induced ERK dimerization. DMSO, used as a drug solvent, had no effect in the formation of dimers. U0126 and PD-0325901 at 10 µM completely prevent ERK dimerization due to their activity upstream of ERK. Low concentrations of DEL-22379 did not have a significant effect, but 10 µM concentration or higher could effectively inhibit ERK dimerization, although the membrane was

not clear enough. Thus, the same experiment was carried using DEL-22379 concentrations between 10 and 20 µM, to further investigate its inhibiting capabilities in that range (**Figure 9**).

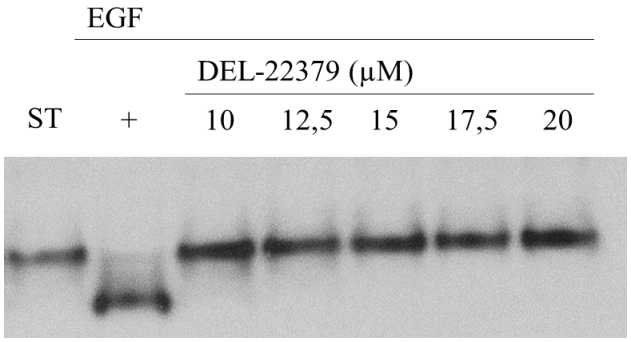

Figure 9. ERK dimerization inhibition by DEL-22379 in A549 cells*. Cells were treated with various concentrations of DEL-22379 to confirm its inhibitory properties. Membrane was incubated with anti-ERK2 primary antibody.*

As it has been previously explained, DEL-22379 can prevent ERK dimerization without changing its phosphorylation state. To check if this was also true for A549 cells, a SDS-PAGE was performed with the same lysates (**Figure 10**). First, the membranes were incubated with a p-ERK primary antibody to examine the phosphorylation state of ERK in the cells. Then, the total levels of ERK1/2 were inspected to verify that a change of intensity of the signal correspond to a lower phosphorylation rate and not to a variation in total protein concentration.

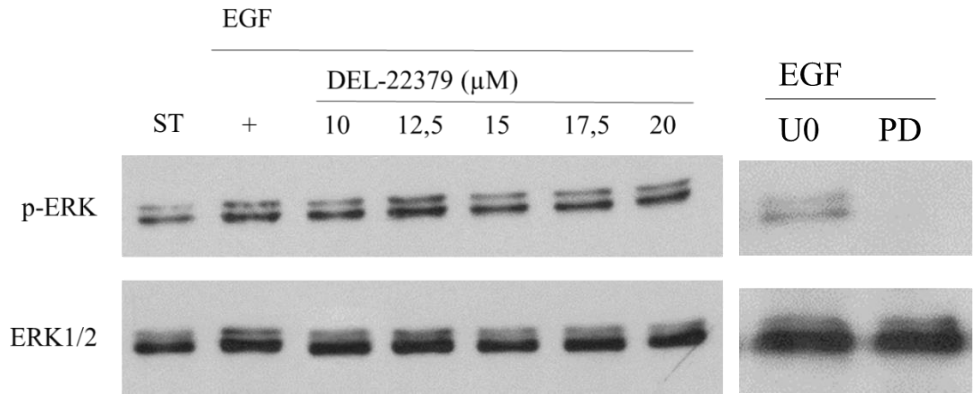

Figure 10. Visualization of ERK phosphorylation (Tyr 204) levels in response to DEL-22379, U0126 and PD-0325901. *ERK phosphorylation was not affected by the treatment with DEL-22379 at different concentrations, while it was lower in cells treated with U0126 and PD-0325901. The ERK1/2 total amount was the same for all the samples.*

The disruption of the formation of ERK dimers implies a greater proportion of ERK monomers in the cell. The activation of the cytoplasmic substrates of ERK requires of ERK dimers, while the nuclear substrates are activated by monomers. Therefore, the inhibition of ERK dimerization would theoretically lower the levels of phosphorylated cytoplasmic substrates while increasing the phosphorylation of nuclear ones because there is more ERK monomer available, as it has been described by Herrero et al. Thus, the phosphorylation state of these substrates was examined in A549 cells treated with DEL-22379 (**Figure 11**). The Ribosomal s6 kinase alpha-1 (RSK-1) was

selected as a cytoplasmatic ERK substrate, while ETS Like-1 protein (ELK-1) was chosen as a nuclear substrate.

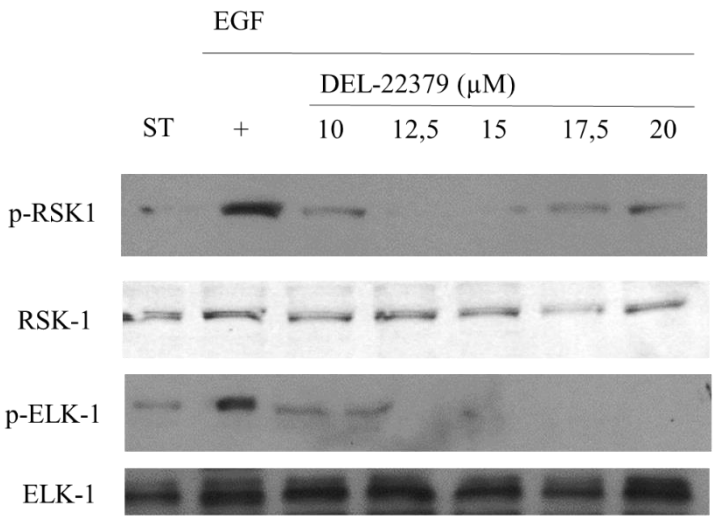

Figure 11. Phosphorylation state variation of ERK substrates in response to DEL-22379 in A549 cells. *Phosphorylation levels of RSK-1 and ELK-1 were considerably lower in DEL treated cells. Total amount of RSK-1 and ELK-1 was the same for every sample.*

RSK-1 and ELK-1 phosphorylation levels were much lower in DEL-22379-treated cells when compared to non-treated cells. While p-RSK1 levels correlate with previous results in colorectal and melanoma cells, p-ELK1 levels are reduced instead of increasing. In order to try to explain this decrease in p-ELK1, the activation of other components of the pathway was checked. MEK and RAF activation was inspected looking at their respective phosphorylation state (**Figure 12**).

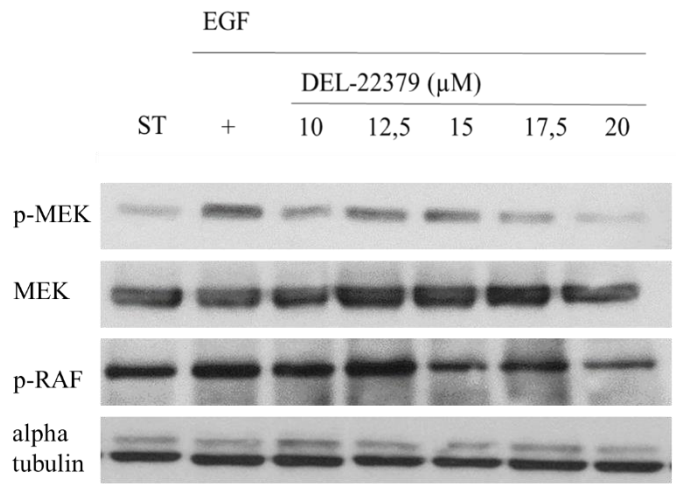

Figure 12. MEK and RAF phosphorylation levels are lower in cells treated with high concentrations of DEL- 22379. Band intensity of MEK was the same for all samples. The measurement of total RAF levels was not possible, so total protein concentration was compared using alpha-tubulin levels.

Phosphorylated MEK showed a slightly lower general levels in DEL-22379-treated cells, showing a more significant decrease at 17,5 and 20 μL. p-RAF also exhibited a reduction of activation state at high DEL-22379 concentrations.

5.2 DEL-22379 IC_{50} calculation in A549 cells

After the molecular characterization of DEL-22379 inhibition in A549 cells, its biological effects on cultured tumour cells were investigated. The cytostatic effects of DEL-22379, U0126 and PD-0325901 were analysed by calculating the half maximal inhibitory concentration (IC_{50}) of each drug in A549 cells, using a viability assay (**Figure 13**). The cells were cultured in a 96-well plate at 3,000 cells per well density. Then, they were treated with a specific concentration of the inhibitor in each well, constituting a gradient. After 24 hours, the viability of the cells was measured using Presto Blue Viability Reagent and spectrophotometry, as described in Materials and Methods.

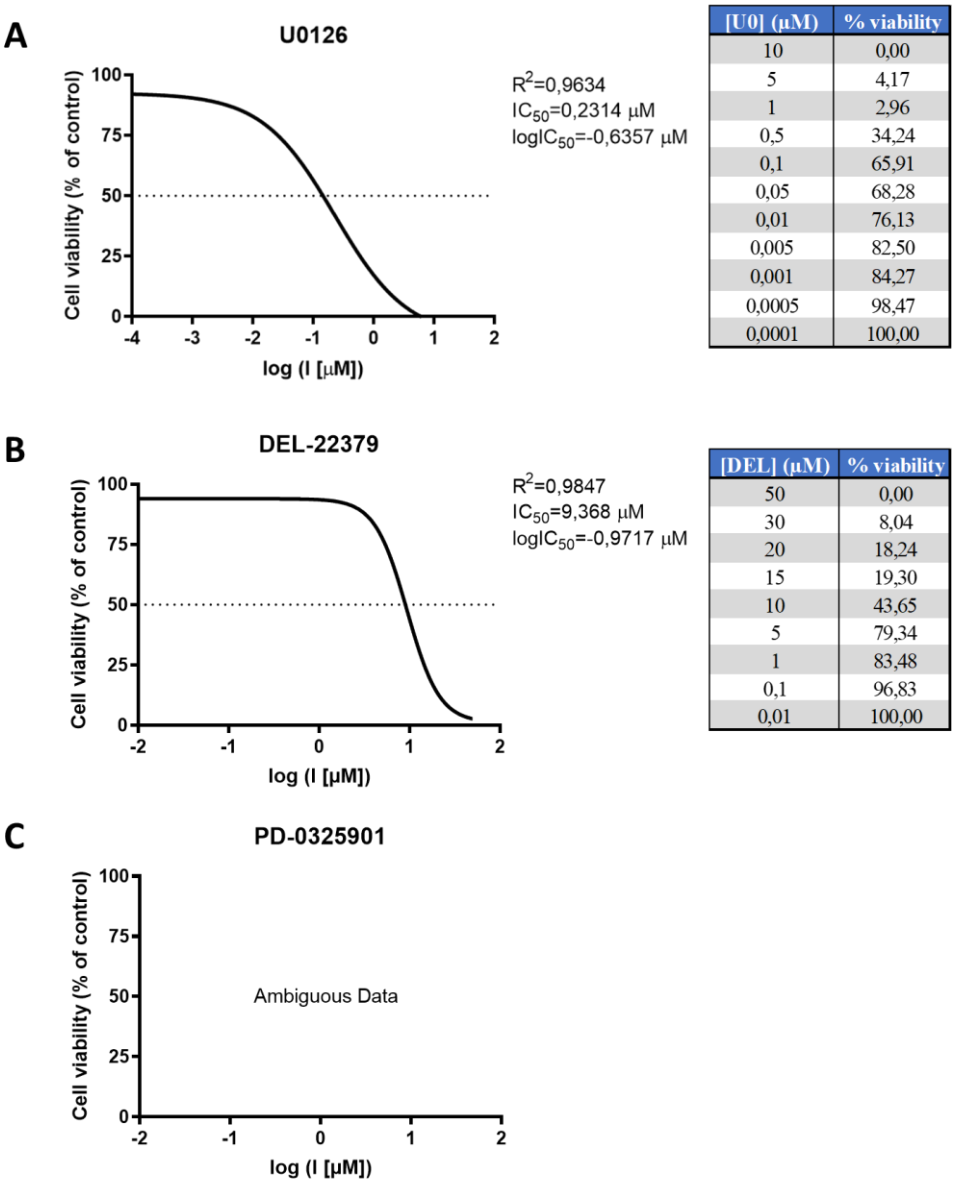

[U0] (µM)	% viability
10	0,00
5	4,17
1	2,96
0,5	34,24
0,1	65,91
0,05	68,28
0,01	76,13
0,005	82,50
0,001	84,27
0,0005	98,47
0,0001	100,00

[DEL] (µM)	% viability
50	0,00
30	8,04
20	18,24
15	19,30
10	43,65
5	79,34
1	83,48
0,1	96,83
0,01	100,00

Figure 13. Results of the IC_{50} calculation. *Graphical representation of the percentage of cell viability normalized to the control(y-axis) vs the logarithmic value of inhibitor concentration (x-*

axis) for U0126 (A), DEL-22379 (B) and PD-0325901(C). The graphics were constructed using the values in the adjacent table to each chart.

A549 cells showed a high sensitivity to the MEK inhibitor U0126 (IC_{50}=0.2314 µM) and a moderate response to DEL-22379 (IC_{50}=9.368 µM). On the other hand, PD-0325901 did not exhibit a good performance in the experiment, minimally reducing cell viability, except for high concentrations.

Considering these results, and examining previous ERK dimerization analysis and immunoblotting, the DEL-22379 concentration selected for following experiments was 10 µM.

5.3 DEL-22379 effectively diminishes cell survival in lung adenocarcinoma cells

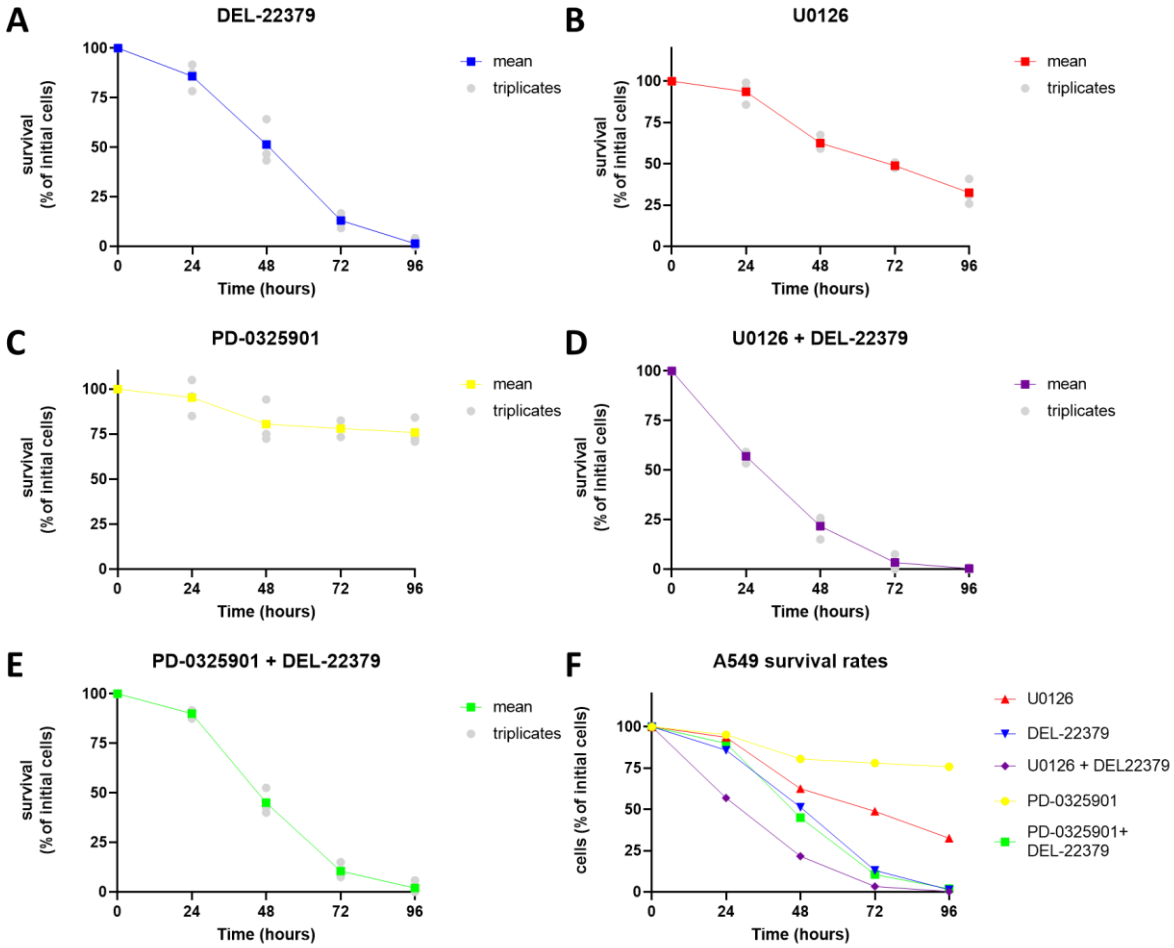

Figure 14. A549 cell survival timelapse for different MAPK inhibitor treatments. *The charts represent the survival rate of A549 cells (normalized to the number of initial cells) (y-axis) for different days (x-axis). All drugs were used at 10 µM final concentration. Five different drug conditions were set, which can be identified by the title of the graphic. The last graphic (F) summarizes all the results for comparation.*

The aim of the next experiment (**Figure 14**) was to observe the effects of each inhibitor in cell survival and proliferation. Therefore, cells were cultured in a 24-well plate at 30.000 cells/well density and treated with a final drug concentration of 10 µM. Five different conditions were set: DEL-22379, U0126, PD-0325901 and the combination of DEL-22379 with the two MEK inhibitors. Every 24 hours, alive cells were counted for each drug condition. A cell survival curve was made with the results.

Surprisingly, DEL-22379 showed a significantly higher survival suppression than U0126, although the last one had a lower IC_{50}, as shown in the preceding experiment. PD-0325901 could prevent cell proliferation, but its effects in cell survival were of little importance, as well as its outcome in combination with DEL-22379. However, the mixture of U016 and DEL-22379 treatment in A549 cells resulted in a great decrease of cell proliferation and survival, showing a synergistic tendency.

5.4 A549 cells migration is reduced by the ERK dimerization inhibitor DEL-22379

Next, the migration and invasion capabilities of A549 cells were tested in a Transwell assay. In these experiments, cells were placed in the top of the porous membrane of a small well (**Figure 15**), which was contained inside a bigger well. Serum-starved cells were able to migrate through the pores in response to a stimulus (5% FBS), which was located into the big well. For the invasion assay, a layer of Matrigel was set over the membrane, simulating the extracellular matrix.

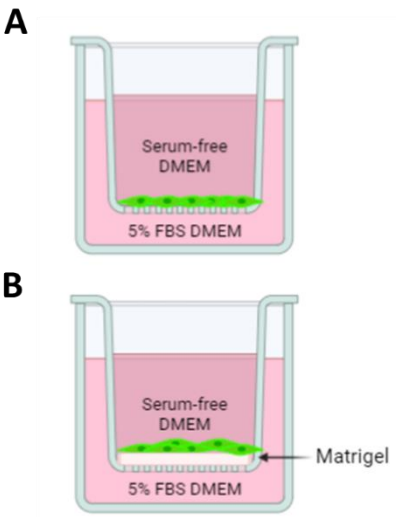

Figure 15. Representation of cell migration (A) and invasion (B) assays. *Cells were cultured in the upper layer of the membrane. A549 cells could migrate through the 0,8 µm pore.*

To get a more precise measurement of cell migration than with other traditional methods, quantification of the cells using confocal fluorescence microscopy was tried. Cells were prepared for microscopy as explained in the technical procedure section. Several pictures of each well were taken (an example of this images can be seen in **Figure 16**). However, quantification of the pictures was not possible due to the curvature of the porous membrane. Because of this curvature, the Z dimension from the microscopy pictures did not correspond with the real position of the cells in the membrane, what made software quantification very problematic. Hence, the fluorescence images were used for illustration purposes, and other quantification technique was performed.

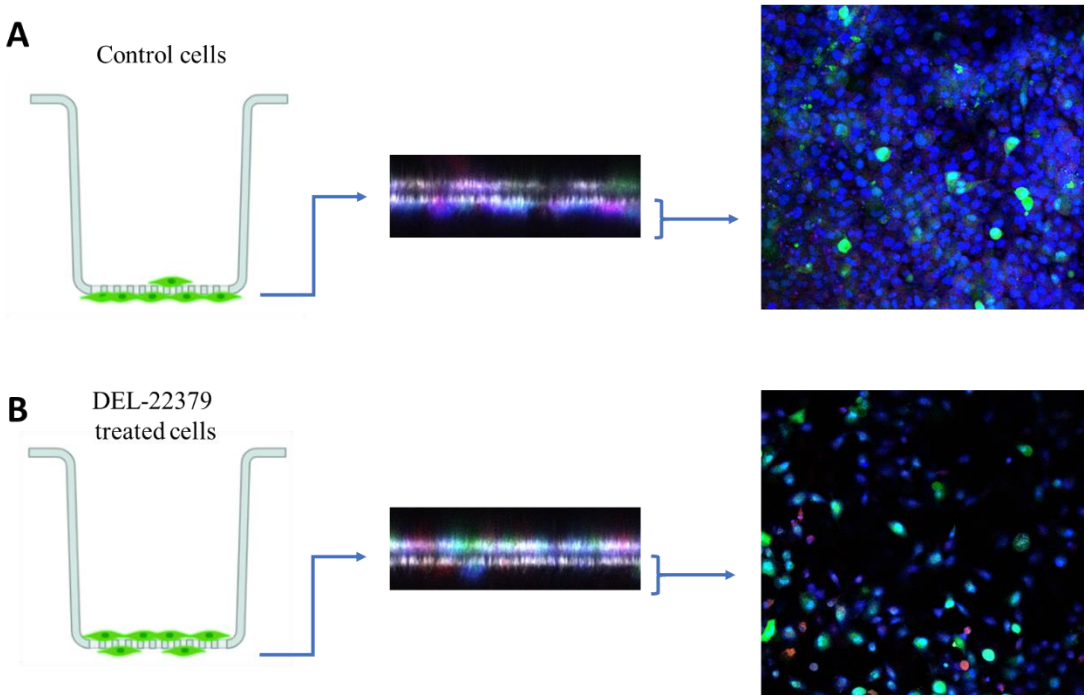

Figure 16. Visualization of cell migration using confocal fluorescence microscopy. *Two conditions are compared in this figure: control cells (A) and DEL-22379 (B). Cells were marked with green, blue, and red fluorophores. For both conditions, a schematic illustration of the wells after the cell migration is represented. Next, and orthogonal view of the two layers of the porous membrane can be seen. Finally, the last images were taken at the lower layer of the membrane. Control cells (A) could easily migrate through the membrane to the lower layer in response to the stimulus, and they could proliferate too. In contrast, DEL-22379 treated cells (B) migration was reduced, so cells remained in the upper layer of the membrane. Few treated cells could migrate to the lower layer.*

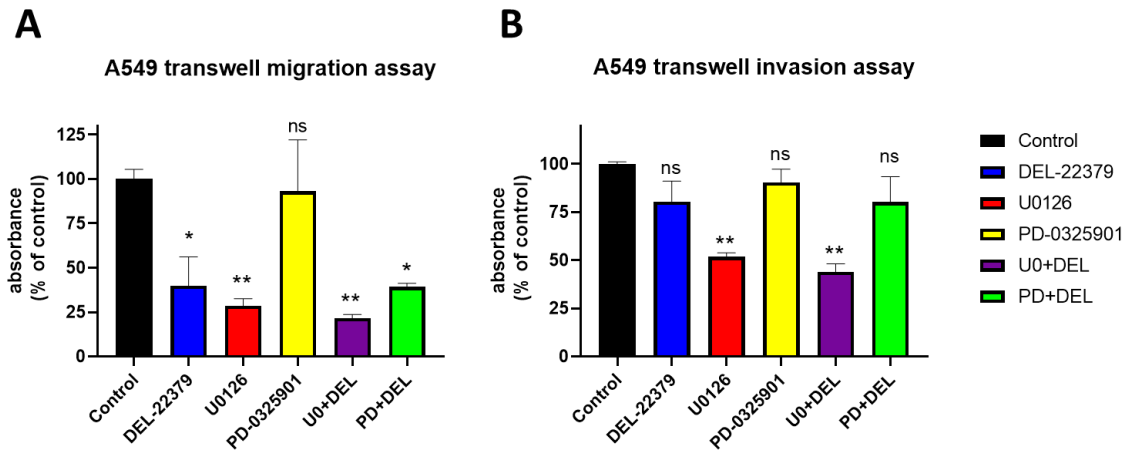

Figure 17. Migratory and invasive response of A549 cells to MAPK inhibitor treatment. *The graphics show the relative (compared to control) absorbance of the acetic acid and methyl violet*

*solution (x-axis) for all the experimental conditions (y-axis). The bar chart represents the average value, and an analysis of variance was performed using a student t-test. * = P-value<0.05. ** = P-value<0.01. ns = non-significant.* ***A)*** *Transwell migration assay.* ***B)*** *Transwell invasion assay. All drugs were used at 10 µM final concentration.*

An alternative quantification method was performed. Thus, A549 cells in the upper layer were removed, and cells in the lower layer were stained using methyl violet. Then, the cells were washed, and the dye was dissolved in an acetic acid solution. Therefore, the more cells migrated to the lower layer of the porous membrane, the more methyl violet was dissolved in this solution. Each sample (two per condition) absorbance was measured in duplicates. This method was used for both migration and invasion assays (**Figure 17**).

A549 cells showed a significant decrease in their migratory function when treated with DEL-22379 and U0126, while PD-0325901 did not exhibit good outcome. The combination of ERK and MEK inhibitor resulted to be the most optimal condition in order to inhibit A549 migration. On the other hand, DEL-22379 was not significantly effective to suppress the invasive behaviour of A549 cells, as well as PD-032591. Only U0126 showed significant results in the invasion assay.

5.5 DEL-22379 reduces tumour growth in the chick embryo model

Finally, to determine the behaviour of lung adenocarcinoma cells *in vivo*, 1.000.000 cells were placed in the chorioallantoic membrane of chick embryos at day 10 of their development, as described in Materials and Methods. Four conditions were established based on former results: control, DEL-22379, U0126 and U0126+DEL-22379. At day 15, tumours were harvested. A significant reduction of tumour weight in the three inhibitor conditions compared with control tumours could be observed (**Figure 18**).

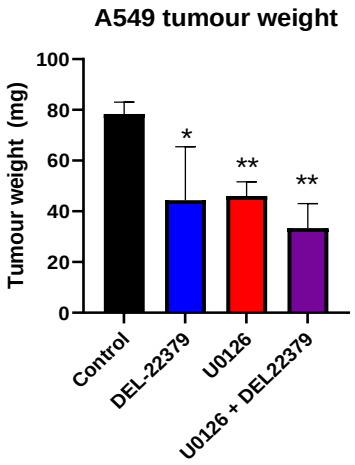

Figure 18. Graphical representation of tumour weight*. Tumours were harvested and weighted. A Student t-test was performed to compare treated tumours with controls. * = P-value<0.05. ** = P-value<0.01.*

A RT-qPCR was performed with genomic DNA samples from brain, CAM, lung, and liver of the chick embryos. Human Alu sequence were amplified from the chick embryo samples and from DNA samples from a known number of A549 cells. However, the values of the chick embryo samples were too low, indicating almost no metastasis even in control tumours.

6. DISCUSSION

ERK dimerization has been established as a good target against tumour progression and oncogenesis (Casar et al., 2008; Herrero et al., 2015; Tomasovic et al., 2020). For this reason, the discovery of new compounds capable of preventing the formation of ERK dimers has become a viable approach to develop new therapeutic strategies. Herrero et al. demonstrated that the ERK inhibitor DEL-22379 had antineoplastic properties in colorectal cancer and melanoma. In addition, this study has explored DEL-22379 therapeutic potential in lung adenocarcinoma with interesting results.

DEL-22379 could inhibit ERK dimerization in A549 lung adenocarcinoma cells without changing ERK phosphorylation. This functional specificity of the inhibitor, which just partially suppresses ERK activity, could mean less side effects when comparing it with other ERK inhibitors. The preservation of ERK phosphorylation would allow usual nuclear activity in normal cells, while the inhibition of dimerization would prevent the oncogenic effects of cytoplasmic substrates in tumour cells. In fact, DEL-22379 exhibited a mild toxicity in several mice experiments (Herrero et al., 2015). In concordance with previous results, the activation of the cytoplasmic ERK substrate RSK-1 was reduced with DEL-22379 treatment. However, the activation of the nuclear substrate ELK-1 also diminished. There are several hypotheses explaining this phenomenon that could be investigated in the future.

First, Tomasovic et al. recently described a new ERK dimerization inhibitor called EDI, which also showed antitumour effects in human colorectal and lung cancer (Tomasovic et al., 2020). As DEL-22379, the treatment with EDI did not affect phosphorylation of the TEY motif (Tyr 204) but reduced the phosphorylation of the threonine 188. They identified the phosphorylation of this residue as necessary for nuclear substrate activation. The inhibition of ERK dimerization prevented the autophosphorylation of the threonine 188 of ERK, which also could be happening in A549 cells. Thus, it would be interesting to analyse the phosphorylation residue in colorectal, melanoma and lung cancer cells to find out the role of this residue in the ERK signalling of cancer cells.

Furthermore, it was noticed that RAF and MEK activation levels were also reduced in DEL-22379-treated cells. This could happen because of various mechanism, like crosstalk with other signalling pathways, the alteration of ERK feedback loops or off-target effects of DEL-22379. Although RAF and MEK activation was lower, phosphorylation of the ERK TEY motif did not change with DEL-22379 treatment, maybe because *RAS* mutant cells have a continuous activation of the pathway, and this does not considerably affect ERK activation. Nonetheless, this could be somehow affecting nuclear substrate phosphorylation. The generation of *ERK* mutant cells unable to bind to DEL-22379 could be useful to discard off-target effects of the drug in RAF, MEK, and

other components of the cascade. There could also be off-target effects in other signalling pathway. If these theoretical mutant cells are treated with DEL-22379 and the same effect in p-ELK1 is observed, it would indicate non-specific interactions.

In vitro, DEL-22379 supressed cancer cell proliferation, survival, and migration. These effects were comparable with the ones induced by the MEK inhibitor U0126, although A549 showed more sensitivity to U0126 in the A549 cell viability and migration assays. Nevertheless, DEL-22379 presented better capabilities to inhibit cell survival, what may happen because of DEL-22379's ability of inducing a significant apoptotic response in *K-RAS* mutant cancer cells (Herrero et al., 2015). Moreover, the combination of both DEL-22379 and U0126 inhibitors was the optimal condition against tumour cells. ERK and MEK inhibitor treatment has been suggested as an effective therapeutic combination (Liu et al., 2018). However, U0126 had not performed well outside the laboratories (Frémin & Meloche, 2010). It would be interesting to test the synergistic behaviour of DEL-22379 with other more clinically successful MEK inhibitors.

Contrarily, PD-0325901 showed almost no effect in any of the experiments. These results corroborate previous findings obtained in other *K-RAS* mutant cancer cells, where PD-0325901 failed to produce a sustained suppression of MAPK pathway signalling (Lito et al., 2014). Their findings imply that drugs that not only decrease the catalytic activity of MEK, but also diminish its reactivation by C-RAF, may be more effective in inhibiting ERK signalling in these cancers. Moreover, PD-0325901 did not performed well in clinical trials with NSCLC patients (Haura et al., 2010). Therefore, these kind of properties of MEK inhibitors should be considered when choosing a DEL-22379 partner in future experiments or clinical trials for *K-RAS* mutant cancers.

DEL-22379 did not perform well in the invasion assay. The number of cells that could reach the lower layer was smaller than in the control, but still not significant. The relative effectiveness of U0126 was also decreased in this experiment. Instead of assuming a lower efficacy of this inhibitors to supress tumour cell invasion, a problem with the quantification technique is more likely to explain these results. The crystal violet method showed enough sensitivity in the migration assay, where cells migrate much more easily than in the invasion conditions. Because of the Matrigel, there is a smaller number of total cells that can invade and migrate to the lower layer of the membrane, what makes quantification more inaccurate. In fact, the absolute absorbance values were approximately ten times lower than in the migration assay. This could explain the lack of significance of the results. Another more sensitive method of quantification should be used for future invasion assays.

The tumour growth of lung adenocarcinoma in chick embryo model was reduced by DEL-22379 and U0126, and the combination of both resulted in a greater reduction. Unfortunately, none of the tumours achieved to metastasise to any of the chick embryo's organs analysed. This could be

resolved by allowing tumour growth and dissemination up to day 17 of development. However, the experiment was conducted with an initial inoculation of one million cancer cells per embryo. This, plus the high growth capacity of this A549 cells, would have likely killed the chick embryo before the day 17. In fact, many of the embryos died during the week of tumour formation (day 10 to day 15). Moreover, in our laboratory, we have previously demonstrated aggressiveness inversely correlates with tumour size in some tumours (García-Ibáñez et al., 2020). Hence, the experiment could be repeated using a smaller number of cells, which could provide enough time for the tumour to metastasise and allow the formation of a measurable tumour mass.

7. CONCLUSIONS

From this work, the following conclusions can be made:

- DEL-22379 can inhibit the formation of ERK dimers in A549 cells without altering the TEY motif phosphorylation.
- Both activation of nuclear and cytoplasmic ERK substrates are lowered by DEL-22379 in lung adenocarcinoma cells.
- DEL-22379 reduces proliferation, survival, and migration of lung adenocarcinoma cells. This reduction is comparable with U0126 inhibition, another MAPK pathway inhibitor.
- DEL-22379 diminishes A549 tumour growth in the chick embryo model.
- DEL-22379 shows a synergistic tendency with MEK inhibitors like U0126 in A549 cells, but not with those unable to maintain signal inhibition in *K-RAS* mutant cells, like PD-0325901.

8. BIBLIOGRAPHY

1. Abdel-Rahman, O. (2016). Targeting the MEK signaling pathway in non-small cell lung cancer (NSCLC) patients with RAS aberrations. *Therapeutic Advances in Respiratory Disease*, *10*(3), 265-274. https://doi.org/10.1177/1753465816632111

2. Anguera, G., & Majem, M. (2018). BRAF inhibitors in metastatic non-small cell lung cancer. *Journal of Thoracic Disease*, *10*(2), 589-592. https://doi.org/10.21037/jtd.2018.01.129

3. Barta, J. A., Powell, C. A., & Wisnivesky, J. P. (2019). Global Epidemiology of Lung Cancer. *Annals of Global Health*, *85*(1). https://doi.org/10.5334/aogh.2419

4. Bethune, G., Bethune, D., Ridgway, N., & Xu, Z. (2010). Epidermal growth factor receptor (EGFR) in lung cancer: An overview and update. *Journal of Thoracic Disease*, *2*(1), 48-51.

5. Boch, C., Kollmeier, J., Roth, A., Stephan-Falkenau, S., Misch, D., Grüning, W., Bauer, T. T., & Mairinger, T. (2013). The frequency of EGFR and KRAS mutations in non-small cell lung cancer (NSCLC): Routine screening data for central Europe from a cohort study. *BMJ Open*, *3*(4). https://doi.org/10.1136/bmjopen-2013-002560

6. Braicu, C., Buse, M., Busuioc, C., Drula, R., Gulei, D., Raduly, L., Rusu, A., Irimie, A., Atanasov, A. G., Slaby, O., Ionescu, C., & Berindan-Neagoe, I. (2019). A Comprehensive Review on MAPK: A Promising Therapeutic Target in Cancer. *Cancers*, *11*(10). https://doi.org/10.3390/cancers11101618

7. Casar, B., & Crespo, P. (2016). ERK Signals: Scaffolding Scaffolds? *Frontiers in Cell and Developmental Biology*, *4*, 49. https://doi.org/10.3389/fcell.2016.00049

8. Casar, B., Pinto, A., & Crespo, P. (2008). Essential role of ERK dimers in the activation of cytoplasmic but not nuclear substrates by ERK-scaffold complexes. *Molecular Cell*, *31*(5), 708-721. https://doi.org/10.1016/j.molcel.2008.07.024

9. Chin, H. M., Lai, D. K., & Falchook, G. S. (2020). Extracellular Signal-Regulated Kinase (ERK) Inhibitors in Oncology Clinical Trials. *Journal of Immunotherapy and Precision Oncology*, *2*(1), 10-16. https://doi.org/10.4103/JIPO.JIPO_17_18

10. Cicchini, M., Buza, E. L., Sagal, K. M., Gudiel, A. A., Durham, A. C., & Feldser, D. M. (2017). Context-Dependent Effects of Amplified MAPK Signaling during Lung Adenocarcinoma Initiation and Progression. *Cell Reports*, *18*(8), 1958-1969. https://doi.org/10.1016/j.celrep.2017.01.069

11. Cox, A. D., Fesik, S. W., Kimmelman, A. C., Luo, J., & Der, C. J. (2014). Drugging the undruggable Ras: Mission possible? *Nature reviews. Drug discovery*, *13*(11), 828-851. https://doi.org/10.1038/nrd4389

12. Crespo, P., & Casar, B. (2016). The Chick Embryo Chorioallantoic Membrane as an in vivo Model to Study Metastasis. *Bio-protocol*, *6*(20), e1962-e1962.

13. Degirmenci, U., Wang, M., & Hu, J. (2020). Targeting Aberrant RAS/RAF/MEK/ERK Signaling for Cancer Therapy. *Cells*, *9*(1). https://doi.org/10.3390/cells9010198

14. Drosten, M., & Barbacid, M. (2020). Targeting the MAPK Pathway in KRAS-Driven Tumors. *Cancer Cell*, *37*(4), 543-550. https://doi.org/10.1016/j.ccell.2020.03.013

15. Duma, N., Santana-Davila, R., & Molina, J. R. (2019). Non-Small Cell Lung Cancer: Epidemiology, Screening, Diagnosis, and Treatment. *Mayo Clinic Proceedings*, *94*(8), 1623-1640. https://doi.org/10.1016/j.mayocp.2019.01.013

16. Fernández-Medarde, A., & Santos, E. (2011). Ras in cancer and developmental diseases. *Genes & Cancer*, *2*(3), 344-358. https://doi.org/10.1177/1947601911411084

17. Frémin, C., & Meloche, S. (2010). From basic research to clinical development of MEK1/2 inhibitors for cancer therapy. *Journal of Hematology & Oncology*, *3*, 8. https://doi.org/10.1186/1756-8722-3-8

18. Fucile, C., Marenco, S., Bazzica, M., Zuccoli, M. L., Lantieri, F., Robbiano, L., Marini, V., Di Gion, P., Pieri, G., Stura, P., Martelli, A., Savarino, V., Mattioli, F., & Picciotto, A. (2015). Measurement of sorafenib plasma concentration by high-performance liquid chromatography in patients with advanced hepatocellular carcinoma: Is it useful the application in clinical practice? A pilot study. *Medical Oncology (Northwood, London, England)*, *32*(1), 335. https://doi.org/10.1007/s12032-014-0335-7

19. García-Ibáñez, Y., Riesco-Eizaguirre, G., Santisteban, P., Casar, B., & Crespo, P. (2020). RAS Subcellular Localization Inversely Regulates Thyroid Tumor Growth and Dissemination. *Cancers*, *12*(9). https://doi.org/10.3390/cancers12092588

20. Guo, Y.-J., Pan, W.-W., Liu, S.-B., Shen, Z.-F., Xu, Y., & Hu, L.-L. (2020). ERK/MAPK signalling pathway and tumorigenesis. *Experimental and Therapeutic Medicine*, *19*(3), 1997-2007. https://doi.org/10.3892/etm.2020.8454

21. Hancock, C. N., Macias, A., Lee, E. K., Yu, S. Y., Mackerell, A. D., & Shapiro, P. (2005). Identification of novel extracellular signal-regulated kinase docking domain inhibitors. *Journal of Medicinal Chemistry*, *48*(14), 4586-4595. https://doi.org/10.1021/jm0501174

22. Haura, E. B., Ricart, A. D., Larson, T. G., Stella, P. J., Bazhenova, L., Miller, V. A., Cohen, R. B., Eisenberg, P. D., Selaru, P., Wilner, K. D., & Gadgeel, S. M. (2010). A Phase II Study of PD-0325901, an Oral MEK Inhibitor, in Previously Treated Patients with Advanced Non–Small Cell Lung Cancer. *Clinical Cancer Research, 16*(8), 2450-2457.

23. Herrero, A., Pinto, A., Colón-Bolea, P., Casar, B., Jones, M., Agudo-Ibáñez, L., Vidal, R., Tenbaum, S. P., Nuciforo, P., Valdizán, E. M., Horvath, Z., Orfi, L., Pineda-Lucena, A., Bony, E., Keri, G., Rivas, G., Pazos, A., Gozalbes, R., Palmer, H. G., … Crespo, P. (2015). Small Molecule Inhibition of ERK Dimerization Prevents Tumorigenesis by RAS-ERK Pathway Oncogenes. *Cancer Cell*, *28*(2), 170-182. https://doi.org/10.1016/j.ccell.2015.07.001

24. Iezzi, A., Caiola, E., Scagliotti, A., & Broggini, M. (2018). Generation and characterization of MEK and ERK inhibitors- resistant non-small-cells-lung-cancer (NSCLC) cells. *BMC Cancer, 18*(1), 1028. https://doi.org/10.1186/s12885-018-4949-6

25. Jaiswal, B. S., Durinck, S., Stawiski, E. W., Yin, J., Wang, W., Lin, E., Moffat, J., Martin, S. E., Modrusan, Z., & Seshagiri, S. (2018). ERK Mutations and Amplification Confer Resistance to ERK-Inhibitor Therapy. *Clinical Cancer Research, 24*(16), 4044-4055. https://doi.org/10.1158/1078-0432.CCR-17-3674

26. Kidger, A. M., Sipthorp, J., & Cook, S. J. (2018). ERK1/2 inhibitors: New weapons to inhibit the RAS-regulated RAF-MEK1/2-ERK1/2 pathway. *Pharmacology & Therapeutics, 187*, 45-60. https://doi.org/10.1016/j.pharmthera.2018.02.007

27. Kohler, J., Catalano, M., & Ambrogio, C. (2018). Back to the Bench? MEK and ERK Inhibitors for the Treatment of KRAS Mutant Lung Adenocarcinoma. *Current Medicinal Chemistry, 25*(5), 558-574. https://doi.org/10.2174/0929867324666170530093100

28. Köhler, J., Zhao, Y., Li, J., Gokhale, P. C., Tiv, H. L., Knott, A. R., Wilkens, M. K., Soroko, K. M., Lin, M., Ambrogio, C., Musteanu, M., Ogino, A., Choi, J., Bahcall, M., Bertram, A. A., Chambers, E. S., Paweletz, C. P., Bhagwat, S. V., Manro, J. R., … Jänne, P. A. (2021). ERK Inhibitor LY3214996-Based Treatment Strategies for RAS-Driven Lung Cancer. *Molecular Cancer Therapeutics, 20*(4), 641-654. https://doi.org/10.1158/1535-7163.MCT-20-0531

29. Li, Y., Zang, H., Qian, G., Owonikoko, T. K., Ramalingam, S. R., & Sun, S.-Y. (2020). ERK inhibition effectively overcomes acquired resistance of epidermal growth factor receptor-mutant non-small cell lung cancer cells to osimertinib. *Cancer, 126*(6), 1339-1350. https://doi.org/10.1002/cncr.32655

30. Lim, S. M., Westover, K. D., Ficarro, S. B., Harrison, R. A., Choi, H. G., Pacold, M. E., Carrasco, M., Hunter, J., Kim, N. D., Xie, T., Sim, T., Jänne, P. A., Meyerson, M., Marto, J. A., Engen, J. R., & Gray, N. S. (2014). Therapeutic targeting of oncogenic K-Ras by a covalent catalytic site inhibitor. *Angewandte Chemie (International Ed. in English)*, *53*(1), 199-204. https://doi.org/10.1002/anie.201307387

31. Lito, P., Saborowski, A., Yue, J., Solomon, M., Joseph, E., Gadal, S., Saborowski, M., Kastenhuber, E., Fellmann, C., Ohara, K., Morikami, K., Miura, T., Lukacs, C., Ishii, N., Lowe, S., & Rosen, N. (2014). Disruption of CRAF-mediated MEK activation is required for effective MEK inhibition in KRAS mutant tumors. *Cancer Cell*, *25*(5), 697-710. https://doi.org/10.1016/j.ccr.2014.03.011

32. Liu, F., Yang, X., Geng, M., & Huang, M. (2018). Targeting ERK, an Achilles' Heel of the MAPK pathway, in cancer therapy. *Acta Pharmaceutica Sinica B*, *8*(4), 552-562. https://doi.org/10.1016/j.apsb.2018.01.008

33. Maemura, K., Shiraishi, N., Sakagami, K., Kawakami, K., Inoue, T., Murano, M., Watanabe, M., & Otsuki, Y. (2009). Proliferative effects of gamma-aminobutyric acid on the gastric cancer cell line are associated with extracellular signal-regulated kinase 1/2 activation. *Journal of Gastroenterology and Hepatology*, *24*(4), 688-696. https://doi.org/10.1111/j.1440-1746.2008.05687.x

34. McCubrey, J. A., Steelman, L. S., Chappell, W. H., Abrams, S. L., Wong, E. WT., Chang, F., Lehmann, B., Terrian, D. M., Milella, M., Tafuri, A., Stivala, F., Libra, M., Basecke, J., Evangelisti, C., Martelli, A. M., & Franklin, R. A. (2007). ROLES OF THE RAF/MEK/ERK PATHWAY IN CELL GROWTH, MALIGNANT TRANSFORMATION AND DRUG RESISTANCE. *Biochimica et biophysica acta*, *1773*(8), 1263-1284. https://doi.org/10.1016/j.bbamcr.2006.10.001

35. Merchant, M., Moffat, J., Schaefer, G., Chan, J., Wang, X., Orr, C., Cheng, J., Hunsaker, T., Shao, L., Wang, S. J., Wagle, M.-C., Lin, E., Haverty, P. M., Shahidi-Latham, S., Ngu, H., Solon, M., Eastham-Anderson, J., Koeppen, H., Huang, S.-M. A., … Junttila, M. R. (2017). Combined MEK and ERK inhibition overcomes therapy-mediated pathway reactivation in RAS mutant tumors. *PLoS ONE*, *12*(10). https://doi.org/10.1371/journal.pone.0185862

36. Myers, D. J., & Wallen, J. M. (2021). Lung Adenocarcinoma. En *StatPearls [Internet]*. StatPearls Publishing. https://www.ncbi.nlm.nih.gov/books/NBK519578/

37. Nagano, T., Tachihara, M., & Nishimura, Y. (2018). Mechanism of Resistance to Epidermal Growth Factor Receptor-Tyrosine Kinase Inhibitors and a Potential Treatment Strategy. *Cells*, *7*(11). https://doi.org/10.3390/cells7110212

38. Pradhan, R., Singhvi, G., Dubey, S. K., Gupta, G., & Dua, K. (2019). MAPK pathway: A potential target for the treatment of non-small-cell lung carcinoma. *Future Medicinal Chemistry*, *11*(8), 793-795. https://doi.org/10.4155/fmc-2018-0468

39. Qi, M., Tian, Y., Li, W., Li, D., Zhao, T., Yang, Y., Li, Q., Chen, S., Yang, Y., Zhang, Z., Tang, L., Liu, Z., Su, B., Li, F., Feng, Y., Fei, K., Zhang, P., Zhang, F., & Zhang, L. (2018). ERK inhibition represses gefitinib resistance in non-small cell lung cancer cells. *Oncotarget*, *9*(15), 12020-12034. https://doi.org/10.18632/oncotarget.24147

40. Rowbotham, S. P., & Kim, C. F. (2014). Diverse cells at the origin of lung adenocarcinoma. *Proceedings of the National Academy of Sciences*, *111*(13), 4745-4746. https://doi.org/10.1073/pnas.1401955111

41. Tomasovic, A., Brand, T., Schanbacher, C., Kramer, S., Hümmert, M. W., Godoy, P., Schmidt-Heck, W., Nordbeck, P., Ludwig, J., Homann, S., Wiegering, A., Shaykhutdinov, T., Kratz, C., Knüchel, R., Müller-Hermelink, H.-K., Rosenwald, A., Frey, N., Eichler, J., Dobrev, D., … Lorenz, K. (2020). Interference with ERK-dimerization at the nucleocytosolic interface targets pathological ERK1/2 signaling without cardiotoxic side-effects. *Nature Communications*, *11*(1), 1733. https://doi.org/10.1038/s41467-020-15505-4

42. Unni, A. M., Harbourne, B., Oh, M. H., Wild, S., Ferrarone, J. R., Lockwood, W. W., & Varmus, H. (2018). Hyperactivation of ERK by multiple mechanisms is toxic to RTK-RAS mutation-driven lung adenocarcinoma cells. *ELife*, *7*. https://doi.org/10.7554/eLife.33718

43. Yap, J. L., Worlikar, S., MacKerell, A. D., Shapiro, P., & Fletcher, S. (2011). Small-molecule inhibitors of the ERK signaling pathway: Towards novel anticancer therapeutics. *ChemMedChem*, *6*(1), 38-48. https://doi.org/10.1002/cmdc.201000354